Journal of Mathematical Modeling and Fractional Calculus
https://acspublisher.com/journals/index.php/jmmfc
Received:16-05-2026, **Revised:** 14-06-2026,
Accepted: 18-06-2024, **Published:** 20-06-2026,
https://doi.org/10.48165/jmmfc.2026.3108, 3(1),148-168.

Analysis and investigation of complex network immunity waning and two strain dynamical system

Aqeel Ahmad[a*]

[a]Department of Mathematics, Ghazi University, D.G. Khan 32200, Pakistan
Corresponding author Email: aqeelahmad.740@gmail.com

Abstract: Some epidemic illnesses, like Zika virus and COVID-19, have several strains of the pathogen, making disease control difficult and leading to complex dynamics. We do not know, however, fully comprehend the dynamic characteristics of interacting numerous strains. Vaccination is the most efficient method of outbreak control since it reduces the actual amount of illnesses and creates herd immunity. In order to do this, we proposed the two-strain epidemic model, which shows that immunity declines in a complex network and vaccination is not flawless. The critical values are then further determined in order to confirm the global stability of each strain dominant equilibrium point. Proposed mathematical model is investigated by bounded solution, positive and unique solution which are major characteristic of the epidemic model. To confirm the rate of spread under different conditions, the verge condition which incorporates sensitivity analysis is also developed. Caputo fractional operator is utilized for numerical solutions under different fractional values. Lastly, the outcomes of the theoretical study have been seen by numerical simulations for the developed solution. Understanding the dynamics and behaviors of multi-strain epidemics is made easier by the current findings.

Keywords: Mathematical modeling, Zika, COVID, Stability, Sensitivity, Newton polynomial.

1. Introduction

1.1. Zika Virus and COVID-19

The Zika virus was first discovered in a Rhesus macaque monkey in Uganda in 1947, and during the 1950s, human infections were reported across several African nations [1]. Between the 1960s and 1980s, sporadic cases were detected in Asia and Africa. However, since 2007, major outbreaks of Zika virus disease have been documented in the Americas, Asia, the Pacific, and Africa. Zika virus infection is primarily transmitted by infected *Aedes* mosquitoes, particularly *Aedes aegypti*, which bite during the day. Additional transmission routes include sexual contact, blood transfusions, organ transplants, and mother-to-fetus transmission during pregnancy.

For individuals who develop symptoms, the illness is typically mild, including fever, rash, conjunctivitis, muscle and joint pain, malaise, and headache. These symptoms usually appear 3–14 days after infection and last 2–7 days [2]. However, Zika virus infection during pregnancy can cause severe congenital abnormalities, including microcephaly, limb contractures, high muscle tone, visual impairments, and hearing loss, collectively termed Congenital Zika Syndrome. Both asymptomatic and symptomatic infections may lead to these outcomes. Furthermore, Zika virus infection is associated with Guillain-Barré syndrome, myelitis, and neuropathy in older children and adults.

Similarly, COVID-19, caused by the severe acute respiratory syndrome coronavirus 2 (SARS-CoV-2), has had a devastating global impact. With over 6 million fatalities worldwide, COVID-19 represents the most significant global health emergency since the 1918 influenza pandemic [3]. The symptoms of COVID-19 range from mild illness to severe respiratory distress, typically appearing 2–14 days after viral exposure. Both influenza and COVID-19 can be detected using nucleic acid amplification tests (NAATs), such as PCR testing. Prevention strategies include frequent handwashing, avoiding touching the face, maintaining physical distance, and using hand sanitizers. Antiviral medications, which reduce the risk of severe illness and death by preventing viral replication, must be prescribed within five to seven days of symptom onset for high-risk individuals.

1.2. Mathematical Modeling of Epidemics

Mathematical modeling is an idealized form of scientific modeling in which an object of study is characterized using mathematical techniques, and research is conducted using mathematical methods. A mathematical model can be defined as a fictitious microworld in which entities behave according to precise rules; mathematics provides a vocabulary to articulate behavioral assumptions in a concise and understandable way, allowing us to predict the future of this hypothetical world and analyze how predictions change if the governing laws are altered [4].

Early epidemic models, such as the classical SIR (Susceptible-Infected-Recovered) framework developed by Kermack and McKendrick [5], used integer-order differential equations and assumed homogeneous mixing, where every individual has an equal probability of contacting an infected person. However, real-world interactions are highly heterogeneous and often exhibit memory effects, meaning that past infections influence future susceptibility and immunity. To address these limitations, fractional-order epidemic models have been developed. Fractional calculus captures the memory and hereditary properties of biological systems more accurately than integer-order models, making it particularly suitable for modeling disease transmission dynamics within complex networks. Recent studies have successfully applied fractional-order models to examine COVID-19 transmission, demonstrating their utility in understanding how interventions such as vaccination and social distancing affect outbreak trajectories. Fractional calculus is the extension of integer order calculus, which primarily studies the arbitrary order differentiation and integration of a function. The fractional derivative definition is related with the entire time domain, while the integer derivative is connected to a specific time, so a fractional order system serves as either long term or short-term memory [6, 7, 8].

A greater memory influence for describing a variety of physical problems can be obtained with fractional calculus [9, 10] . Because fractional operators have memory and genetic characteristics, they can be used to better the realism of the model. By retaining all previous data, the memory properties of the fractional models helps in the translation of the infectious disease models more accurately [11, 12]. When we deal with fractional order operators, the involvement of memory and hereditary characteristics offers a much more realistic way to model disease. The fractional order models preserve all past information because of the memory property that helps to predict the mathematical models more precisely. We have noticed clearly that modeling of real world and physical situations with the non integer - order operators is much more accurate as compared to the classical derivative framework [13, 14].

The applications of mathematical models with Caputo operator in some recent articles depict the stability analysis, existence of single solution and the superiority of Caputo operator on traditional model through numerical simulations. The complex and chaotic dynamics of the spread of diseases were not adequately captured by traditional models, as evidenced by recent papers in the field of epidemiology. Rather, real epidemic data mostly from dependable sources like the WHO was utilized to validate and validate the Caputo versions. Moreover, a clear image of the reproduction number is obtained when we apply Caputo's operator to analyze the disease's pattern under numerous biological parameter values. The preference of Caputo operator over other fractional operators is for various reasons: it is a best suitable for system with initial values, it approaches to the classical operator when fractional value tends to integer value, consistency with classical derivatives, smoothness and satisfying Convolution principle. Consider for instance, [15, 16] and the research papers cited within.

In this work, we focus on a two-strain epidemic model that incorporates imperfect vaccination and waning immunity within a complex network framework. Two-strain models are essential for studying diseases with multiple variants, such as Zika virus and COVID-19, because different strains may exhibit distinct transmission rates, infection periods, immunity periods, and cross-immunity profiles [17]. By analyzing the stability of disease-free equilibrium, strain-dominance equilibrium, and coexistence equilibrium, we aim to provide insights into how imperfect vaccines and network structure influence the long-term dynamics of multi-strain epidemics.

2. Two Strain Model

The variability of population interaction on epidemic dynamics may be described by modeling the entire population as a social network. A person is seen as a node in the intricate network. Furthermore, in a complicated network, the interaction between two people is comparable to an edge connecting two nodes. The amount of edges that a node links determines its degree. All nodes are categorized into n categories based on their level in the social network. Group K's population consists of several state variables:

2.1. Description of compartments

$S_K(t)$ indicates the strength of susceptible nodes. $V_K(t)$ represents the strength of the two strains' vaccinated nodes. For strain I, $I_K(t)$ represents the intensity of the infected nodes. For strain J, $J_K(t)$ represents the severity of the infected nodes. $R_K(t)$ indicates how strongly nodes were recovered.

2.2. Description of Parameters

The birth ratio is represented by τ. The ratio of natural mortality is represented by ω. ε denotes the immunization rate. The likelihood of infection upon coming into touch with an infected individual with strain I is represented by μ_1. The likelihood of infection upon coming into touch with an infected individual with strain J is represented by μ_2. The infection ratio of those who received the vaccination with strain I is represented by μ_3. Vaccinated individuals' infection ratio with strain J is represented by μ_4. The chance of recovery for strain I is represented by μ_5. The likelihood of recovery for strain J is represented by μ_6. The chance of infection caused by strain I is represented by κ_1. The likelihood of infection caused by strain J is represented by κ_2. The likelihood of recovery for strain I is represented by μ_6. A vaccine's passing rate, or β_1, indicates that protection diminishes with time. β_2 is the coefficient of natural immune protection.

Moreover, we established $\theta_1 = \varepsilon + \omega$, $\theta_2 = \mu_5 + \kappa_1 + \omega$ and $\theta_3 = \mu_6 + \kappa_2 + \omega$. Assume that every parameter is positive. In the dynamics of all subsystems, the linked functions $\phi_1(t)$ and $\phi_2(t)$ are represented as follows: $\phi_1(t) = \sum_{H=1}^{n} I_H(t)$ and $\phi_2(t) = \sum_{H=1}^{n} andQ(H|K)Q(H|K)J_H(t)$. The conditional probability that a node with degree K is in contact with a node with degree H is defined as $Q(H|K)$. The likelihood of being linked to a node of degree H in non-correlated networks is $HQ(H)$. Consequently, $Q(H|K) = HQ(H)/ < K >$, where the mean degree of the whole network is $< K >= \sum_{H=1}^{n} HQ(H)$. After taking into account the uncorrelated networks in this study, $\phi_1(t)$ and $\phi_2(t)$ may be defined as follows: $\phi_1(t) = \frac{\sum_{H=1}^{n} Q(H)I_H(t)}{<K>}$ .The formula is $\phi_2(t) = \frac{\sum_{H=1}^{n} Q(H)J_H(t)}{<K>}$. The total number of people is thus N_K, where $K = 1,2,3,.....,n$. The maximum degree is n. As a result, the total population is $N = N_1 + N_2 + ...N_n$. We use the network, which has the degree $Q(K)$ and indicates the percentage of randomly chosen nodes of degree K, and $Q(K) = \frac{N_K}{N}$ to account for the contact heterogeneity. Ordinary differential equations with K sub-systems comprise the dynamic model (Wu et.al., 2024):

$$\begin{aligned}
\mathbb{D}S_K(t) &= \tau + \beta_1 V_K + \beta_2 R_K - (\mu_1 K\phi_1 + \mu_2 K\phi_2 + \theta_1)S_K, \\
\mathbb{D}V_K &= \varepsilon S_K - (\omega + \mu_3 K\phi_1 + \mu_4 K\phi_2 + \beta_1)V_K, \\
\mathbb{D}I_K(t) &= \mu_1 K S_K \phi_1 + \mu_3 K V_K \phi_1 - \theta_2 I_K, \\
\mathbb{D}J_K(t) &= \mu_2 K S_K \phi_2 + \mu_4 K V_K \phi_2 - \theta_3 J_K, \\
\mathbb{D}R_K(t) &= \mu_5 I_K + \mu_6 J_K - (\omega + \beta_2)R_K.
\end{aligned} \tag{1}$$

Here the conditions $S_K(0) = S_K^0, V_K = V_K^0, I_K = I_K^0, J_K = J_K^0, R_K = R_K^0$ are all non-negative. Using Caputo operator the new developed model is:

$$\begin{aligned}
{}^{C}\mathbb{D}_t^{\omega_1} S_K(t) &= \tau + \beta_1 V_K + \beta_2 R_K - (\mu_1 K\phi_1 + \mu_2 K\phi_2 + \theta_1)S_K, \\
{}^{C}\mathbb{D}_t^{\omega_1} V_K &= \varepsilon S_K - (\omega + \mu_3 K\phi_1 + \mu_4 K\phi_2 + \beta_1)V_K, \\
{}^{C}\mathbb{D}_t^{\omega_1} I_K(t) &= \mu_1 K S_K \phi_1 + \mu_3 K V_K \phi_1 - \theta_2 I_K, \\
{}^{C}\mathbb{D}_t^{\omega_1} J_K(t) &= \mu_2 K S_K \phi_2 + \mu_4 K V_K \phi_2 - \theta_3 J_K, \\
{}^{C}\mathbb{D}_t^{\omega_1} R_K(t) &= \mu_5 I_K + \mu_6 J_K - (\omega + \beta_2)R_K.
\end{aligned} \tag{2}$$

Here the conditions $S_K(0) = S_K^0$, $V_K = V_K^0$, $I_K = I_K^0$, $J_K = J_K^0$, $R_K = R_K^0$ are all non-negative.

3. Mathematical analysis

In this section, we aim to provide comprehensive mathematical analysis for the suggested model including equilibrium points, stability, reproductive number and sensitivity.

3.1. Existence of equilibrium points

To find the equilibrium points, the system of equations is equal to zero. Four stable states are present in the model (3.1.2), including two endemic equilibrium points, one coexistence equilibrium point, and one disease-free equilibrium point. First, we establish the following guidelines:

$$\begin{aligned} \nu_1 &= \mu_1 K\phi_1 + \mu_2 K\phi_2 + \theta_1, \\ \nu_2 &= \omega + \beta_1 + \mu_3 K\phi_1 + \mu_4 K\phi_2, \\ \nu_3 &= \frac{\theta_3\mu_5(\mu_1 K\nu_2 + \varepsilon\mu_3 K)\phi_1 + \theta_2\mu_6(\mu_2 K\nu_2 + \varepsilon\mu_4 K)\phi_2}{\theta_2\theta_3\nu_1\nu_2}, \\ \chi &= \frac{\tau\nu_1\nu_2(\omega+\beta_2)}{(\nu_1\nu_2 - \omega\beta_1)(\omega+\beta_2) - \beta_2\nu_1\nu_2\nu_3}. \end{aligned}$$

Besides, the equilibrium points can be made:

$$S_K = \frac{\chi}{\nu_1}, V_K = \frac{\varepsilon\chi}{\nu_1\nu_2}, I_K = \frac{\chi(\mu_1 K\nu_2 + \varepsilon\mu_3 K)\phi_1}{\theta_2\nu_1\nu_2}, J_K = \frac{\chi(\mu_2 K\nu_2 + \varepsilon\mu_4 K)\phi_2}{\theta_3\nu_1\nu_2}. \tag{3}$$

Consequently, it may be seen as follows:

- The balance points without illness: $E_0 = (S_K^0, V_K^0, I_K^0, J_K^0)$ with $\phi_1 = 0, \phi_2 = 0$;
- The endemic strain balance I: $E_1 = (S_K^1, V_K^1, I_K^1, J_K^1)$ with $\phi_1 > 0, \phi_2 = 0$;
- The endemic strain balance J: $E_2 = (S_K^2, V_K^2, I_K^2, J_K^2)$ with $\phi_1 = 0, \phi_2 > 0$;
- The coexistence equilibrium: $E_\diamond = (S_K^\diamond, V_K^\diamond, J_K^\diamond)$ with $\phi_1 > 0, \phi_2 > 0$.

Substituting relation I_k, J_k into expression $\phi_1(t), \phi_2(t)$ we can conclude

$$\phi_1 = \frac{\chi\phi_1}{\theta_2(K)} \sum_{H=1}^{n} \frac{\mu_1 H^2 Q(H)\nu_2 + \varepsilon\mu_3 H^2 Q(H)}{\nu_1\nu_2},$$

$$\phi_2 = \frac{\chi\phi_2}{\theta_3(K)} \sum_{H=1}^{n} \frac{\mu_2 H^2 Q(H)\nu_2 + \varepsilon\mu_4 H^2 Q(H)}{\nu_1\nu_2}.$$

After that,

$$a_1(\phi_1,\phi_2) = \frac{\chi\phi_1}{\theta_2(K)} \sum_{H=1}^{n} \frac{\mu_1 H^2 Q(H)\nu_2 + \varepsilon\mu_3 H^2 Q(H)}{\nu_1\nu_2} - 1,$$

$$a_2(\phi_1,\phi_2) = \frac{\chi\phi_2}{\theta_3(K)} \sum_{H=1}^{n} \frac{\mu_2 H^2 Q(H)\nu_2 + \varepsilon\mu_4 H^2 Q(H)}{\nu_1\nu_2} - 1.$$

The aforementioned formula may be solved as follows:

$$\phi_1 a_1(\phi_1,\phi_2) = 0, \quad \phi_2 a_2(\phi_1,\phi_2) = 0.$$

The equilibrium points and the fundamental reproduction number are then examined as follows.

- $(\phi_1, \phi_2) = (0, 0)$. is the constant solution of model (3.1.2). The connection $I_K = 0, J_K = 0$ may be inferred, indicating the existence of a disease-free equilibrium E_0.

- To determine the strain I's endemic equilibrium E_1, we assume that it corresponds to a pair of solutions (ϕ_1, ϕ_2), where $\phi_1 > 0, \phi_2 = 0$. A positive solution of $a_1(\phi_1, 0) = 0$ must be discovered in order to determine the solution of ϕ_1. In light of the study above, we have

$a_1(\phi_1, 0) = 0$ Given that $a_1(1,0) \leq 0$ and $\frac{\partial a_1(\phi_1,0)}{\partial \phi_1} < 0$ and also beccause $a_1(0,0) > 0$
We can obtain that there is an only $\overline{\phi_1} \in (0,1)$. such that$a_1(\overline{\phi_1}, 0) = 0$ using the theorem of intermediate values, which is comparable to

$$\mathbf{R}_1 = \frac{(\mu_1(\omega+\beta_1)+\varepsilon\mu_3) < K^2 >}{\theta_2\theta_1(\omega+\beta_1) < K >} > 1. \tag{4}$$

where $\sum_H^n H^2 Q(H) = < K^2 >$. The correlation $I_K \neq 0, J_K \leq 0$, suggests that strain I is in an endemic equilibrium. Similarly, we can show the coexistence equilibrium $E_\diamond$ and the endemic equilibrium E_2 of strain J using the intermediate value theorem, which completes the proof. As a result, it has

$$\mathbf{R}_2 =: \frac{(\mu_2(\omega+\beta_1)+\varepsilon\mu_4) < K^2 >}{\theta_3\theta_1(\omega+\beta_1) < K >} > 1. \tag{5}$$

In conclusion, we have the following observations:
Remark 1: We may conclude that equilibrium points of strains 1 and 2 occur when $\mathbf{R}_1 > 1$ and $\mathbf{R}_2 >1$ correspondingly, based on the components of the equilibrium points E_1 and E_2, respectively.
Remark 2: From the elements of the equilibrium point $E_\diamond$, we may infer that when $\mathbf{R}_1 > 1$ and $\mathbf{R}_2 > 1$, the coexistence equilibrium point is reached.

3.2. The analysis of sensitivity

Here we have 2 reproductive numbers;

$$\mathbf{R}_1 = \frac{(\mu_1(\omega+\beta_1)+\varepsilon\mu_3) < K^2 >}{\theta_2\theta_1(\omega+\beta_1) < K >}$$

$$\mathbf{R}_2 = \frac{(\mu_2(\omega+\beta_1)+\varepsilon\mu_4) < K^2 >}{\theta_3\theta_1(\omega+\beta_1) < K >}$$

To ascertain the sensitivity of $\mathbf{R}_1$ and $\mathbf{R}_2$, compute the partial derivatives of the threshold for the subsequent parameters.
Case 1 for $\mathbf{R}_1$:
We have;

$$\frac{\partial \mathbf{R}_1}{\partial \mu_1} = \frac{1}{\theta_1\theta_2} > 0,$$

$$\frac{\partial \mathbf{R}_1}{\partial \omega} = \frac{\mu_1}{\theta_1\theta_2(\beta_2+\omega)} - \frac{\mu_1(\beta_2+\omega)+\mu_3\varepsilon}{\theta_1\theta_2(\beta_2+\omega)^2} < 0,$$

$$\frac{\partial \mathbf{R}_1}{\partial \beta_2} = \frac{\mu_1}{\theta_1\theta_2(\beta_2+\omega)} - \frac{\mu_1(\beta_2+\omega)+\mu_3\varepsilon}{\theta_1\theta_2(\beta_2+\omega)^2} < 0,$$

$$\frac{\partial \mathbf{R}_1}{\partial \varepsilon} = \frac{\mu_3}{\theta_1\theta_2(\beta_2+\omega)} > 0,$$

$$\frac{\partial \mathbf{R}_1}{\partial \mu_3} = \frac{\varepsilon}{\theta_1\theta_2(\beta_2+\omega)} > 0,$$

$$\frac{\partial \mathbf{R}_1}{\partial \theta_1} = -\frac{\mu_1(\beta_2+\omega)+\mu_3\varepsilon}{\theta_1^2\theta_2(\beta_2+\omega)} < 0,$$

$$\frac{\partial \mathbf{R}_1}{\partial \theta_2} = -\frac{\mu_1(\beta_2+\omega)+\mu_3\varepsilon}{\theta_1\theta_2^2(\beta_2+\omega)} < 0,$$

Using appropriate parametric parameters, we observe that $\mathbf{R}_0$, is sensitive.

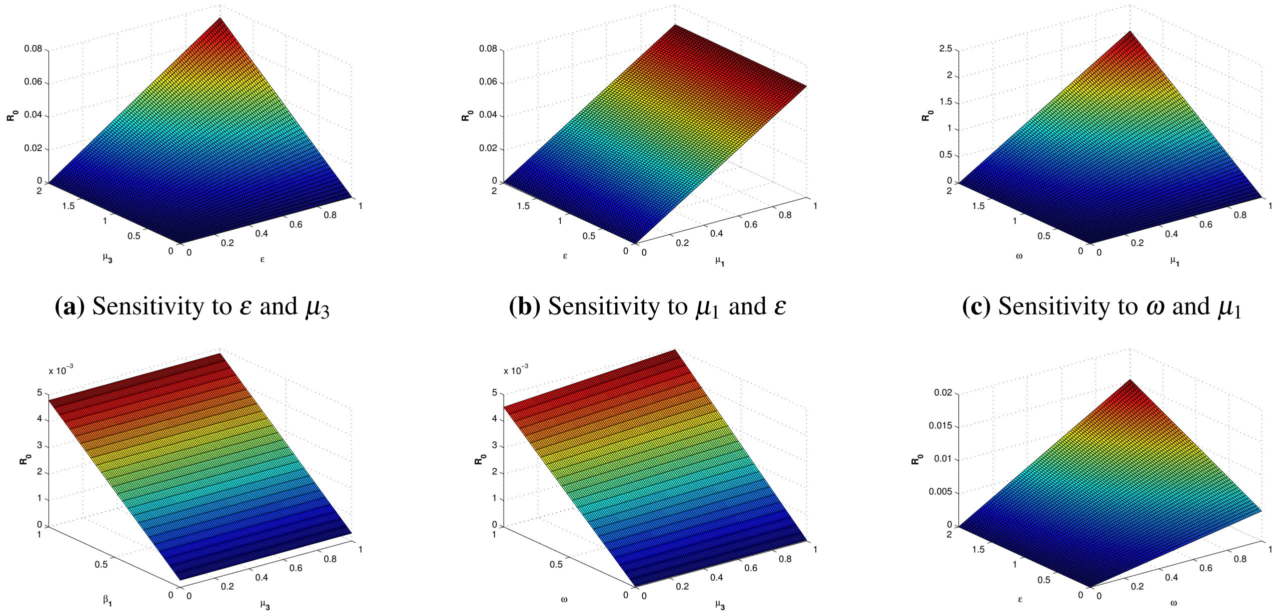

(a) Sensitivity to ε and μ_3 **(b)** Sensitivity to μ_1 and ε **(c)** Sensitivity to ω and μ_1

(d) Sensitivity to μ_3 and β_1 **(e)** Sensitivity to ω and μ_3 **(f)** Sensitivity toω and ε

Figure 1

Case 2 for $\mathbf{R}_2$:

We have;

$$\begin{aligned}
\frac{\partial \mathbf{R}_2}{\partial \mu_2} &= \frac{1}{\theta_1\theta_3} > 0,\\
\frac{\partial \mathbf{R}_2}{\partial \omega} &= \frac{\mu_2}{\theta_1\theta_3(\beta_2+\omega)} - \frac{\mu_2(\beta_2+\omega)+\mu_4\varepsilon}{\theta_1\theta_3(\beta_2+\omega)^2} < 0,\\
\frac{\partial \mathbf{R}_2}{\partial \beta_2} &= \frac{\mu_2}{\theta_1\theta_3(\beta_2+\omega)} - \frac{\mu_2(\beta_2+\omega)+\mu_4\varepsilon}{\theta_1\theta_3(\beta_2+\omega)^2} < 0,\\
\frac{\partial \mathbf{R}_2}{\partial \varepsilon} &= \frac{\mu_4}{\theta_1\theta_3(\beta_2+\omega)} > 0,\\
\frac{\partial \mathbf{R}_2}{\partial \mu_4} &= \frac{\varepsilon}{\theta_1\theta_3(\beta_2+\omega)} > 0,\\
\frac{\partial \mathbf{R}_2}{\partial \theta_1} &= -\frac{\mu_2(\beta_2+\omega)+\mu_4\varepsilon}{\theta_1^2\theta_3(\beta_2+\omega)} < 0,\\
\frac{\partial \mathbf{R}_2}{\partial \theta_3} &= -\frac{\mu_2(\beta_2+\omega)+\mu_4\varepsilon}{\theta_1\theta_3^2(\beta_2+\omega)} < 0.
\end{aligned}$$

Using appropriate parametric parameters, we observe that $\mathbf{R}_0$, is sensitive.

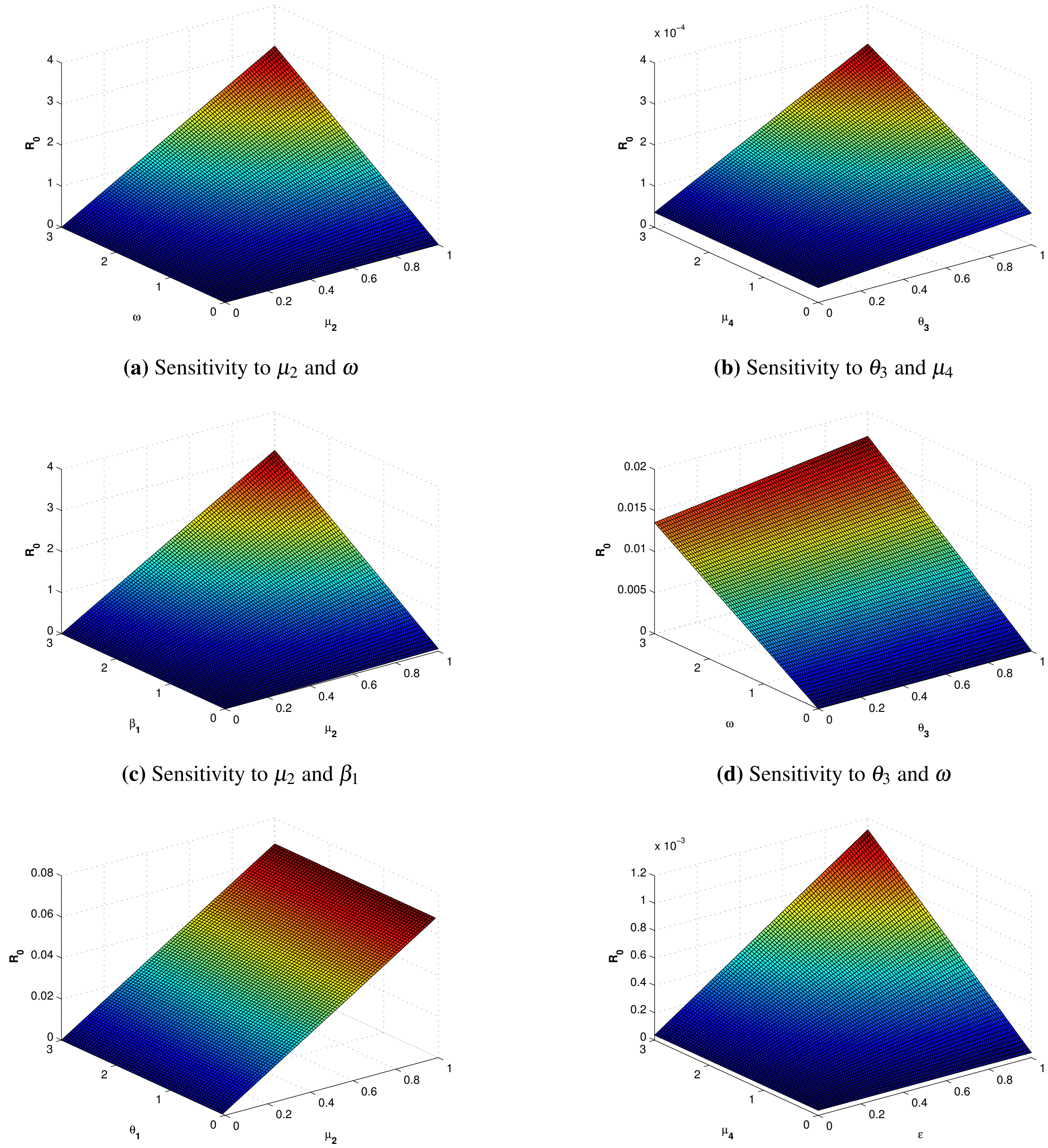

(a) Sensitivity to μ_2 and ω

(b) Sensitivity to θ_3 and μ_4

(c) Sensitivity to μ_2 and β_1

(d) Sensitivity to θ_3 and ω

(e) Sensitivity to θ_1 and μ_2

(f) Sensitivity to μ_4 and ε

Figure 2

3.3. Existence and uniqueness via Caputo Operator

If we are positive that a solution exists, we can use numerical techniques to approximate it. A fractional derivative in the Caputo sense for $0 < \omega_1 \leq 1$ can be used to generalize system (3.1.2).
Let;

$$\lambda_1(t, S_K) = \tau + \beta_1 V_K + \beta_2 R_K - (\mu_1 K \phi_1 + \mu_2 K \phi_2 + \theta_1) S_K,$$

$$\lambda_2(t, V_K) = \varepsilon S_K - (\omega + \mu_3 K \phi_1 + \mu_4 K \phi_2 + \beta_1) V_K,$$

$$\lambda_3(t, I_K) = \mu_1 K S_K \phi_1 + \mu_3 K V_K \phi_1 - \theta_2 I_K, \tag{6}$$

$$\lambda_4(t,J_K)=\mu_2KS_K\phi_2+\mu_4KV_K\phi_2-\theta_3J_K,$$

$$\lambda_5(t,R_K)=\mu_5I_K+\mu_6J_K-(\omega+\beta_2)R_K.$$

By using the initial conditions and fractional integral, we get;

$$S_K(t)=S_{K_0}+\frac{1}{\Gamma(\omega_1)}\int_0^t(t-g)^{\omega_1-1}\lambda_1(t,S_K)dg,$$

$$V_K(t)=V_{K_0}+\frac{1}{\Gamma(\omega_1)}\int_0^t(t-g)^{\omega_1-1}\lambda_2(t,V_K)dg,$$

$$I_K(t)=I_{K_0}+\frac{1}{\Gamma(\omega_1)}\int_0^t(t-g)^{\omega_1-1}\lambda_3(t,I_K)dg, \tag{7}$$

$$J_K(t)=J_{K_0}+\frac{1}{\Gamma(\omega_1)}\int_0^t(t-g)^{\omega_1-1}\lambda_4(t,J_K)dg,$$

$$R_K(t)=R_{K_0}+\frac{1}{\Gamma(\omega_1)}\int_0^t(t-g)^{\omega_1-1}\lambda_5(t,R_K)dg.$$

Let;

$$\lambda(t)=\begin{cases}S_K(t)\\V_K(t)\\I_K(t)\\J_K(t)\\R_K(t)\end{cases},\lambda_0=\begin{cases}S_{K_0}\\V_{K_0}\\I_{K_0}\\J_{K_0}\\R_{K_0}\end{cases},\aleph(g,\lambda(g)=\begin{cases}\lambda_1(t,S_K),\\\lambda_2(t,V_K),\\\lambda_3(t,I_K),\\\lambda_4(t,J_K),\\\lambda_5(t,R_K).\end{cases} \tag{8}$$

So, system (3.4.7) becomes;

$$\lambda(t)=\lambda_0+\frac{1}{\Gamma(\omega_1)}\int_0^t(t-g)^{\omega_1-1}\aleph(g,\lambda(g)dg.$$

Now assume a Banach space $\wp[0,\mathbb{T}]=\nu$ with a norm:

$$\|S_K,V_K,I_K,J_K,R_K\|=\max_{t\in[0,\mathbb{T}]}[|S_K,V_K,I_K,J_K,R_K|].$$

Consider a mapping that is specified as $\nabla:\nu\to\nu$;

$$\nabla\lambda(t)=\lambda_0+\frac{1}{\Gamma(\omega_1)}\int_0^t(t-g)^{\omega_1-1}\aleph(g,\lambda(g)dg.$$

Then, we apply the following assumptions on a non linear function:
P1) There are constants $\iota_b,\iota_b>0$ such that;

$$|\aleph(t,\lambda(t)|\leq\iota_b|\lambda(t)|+\iota_b. \tag{9}$$

P2) There are constants $\beta_b>0$ for each $\lambda,\bar{\lambda}\in\nu$ such that;

$$|\aleph(t,\bar{\lambda})-\aleph(t,\bar{\lambda}_1)|\leq\beta_b|\bar{\lambda}-\bar{\lambda}_1|. \tag{10}$$

Theorem 3.1: If $(P1)$ is true, then there is at least one solution for system (3.1.2).
Proof: Let $\Psi=\{\lambda\in\Psi|\kappa\geq\|\lambda\|\}$ to show that ∇ is limited.

$$\kappa\geq\max_{t\in[0,\mathbb{T}]}\frac{\lambda_0+\left(\frac{\iota_b\mathbb{T}^{\omega_1}}{\Gamma(\omega_1+1)}\right)}{1-\left(\frac{\iota_b\mathbb{T}^{\omega_1}}{\Gamma(\omega_1+1)}\right)}.$$

represents a closed and convex subset of u. Right now;

$$\|\nabla\lambda\| = \max_{t\in[0,\mathbb{T}]} |\lambda_0 + \frac{1}{\Gamma(\omega_1)}\int_0^t (t-g)^{\omega_1-1}\aleph(g,\lambda(g)dg|,$$

$$\leq |\lambda_0| + \frac{1}{\Gamma(\omega_1)}\int_0^t (t-g)^{\omega_1-1}|\aleph(g,\lambda(g)|dg,$$

$$\leq |\lambda_0| + \frac{1}{\Gamma(\omega_1)}\int_0^t (t-g)^{\omega_1-1}[\iota_b|\lambda(g)|+\iota_b]dg,$$

$$\leq |\lambda_0| + [\iota_b\|\lambda\|+\iota_b]\frac{\mathbb{T}^{\omega_1}}{\Gamma(\omega_1++1)} \leq \kappa.$$

Since $\lambda \in \Psi \Rightarrow \nabla(\Psi) \subseteq \Psi$, it shows that ∇ is bounded. Let $t_1 < t_2 \in [0,\mathbb{T}]$, To demonstrate that ∇ is entirely continuous, consider;

$$\begin{aligned}
\|\nabla\lambda(t_2) - \nabla\lambda(t_1)\| &= |\frac{1}{\Gamma(\omega_1)}\int_0^{t_2}(t_2-g)^{\omega_1-1}\aleph(g,\lambda(g)dg \\
&- \frac{1}{\Gamma(\omega_1)}\int_0^{t_1}(t_1-g)^{\omega_1-1}\aleph(g,\lambda(g)dg|, \\
&\leq [\iota_b\|\lambda\|+\iota_b]\frac{[t_2^{\omega_1}-t_1^{\omega_1}]}{\Gamma(\omega_1+1)}.
\end{aligned}$$

This means that $t_2 \to t_1$ equals $\|\nabla\lambda(t_2) - \| \to 0$. The continuous nature of operator ∇ is shown by the Arzela-Ascoli theorem. Both the Banach fixed point theorem and Schauder's fixed point theorem show that system (3.1.2) has a unique solution and at least one solution, respectively.

Theorem 3.2: The system (3.1.2) is assumed to have a unique solution if the conditions $(P2)$ are satisfied.

Proof: Let $\bar{\lambda}, \bar{\lambda}_1 \in \beta$. Take;

$$\begin{aligned}
\|\nabla(\bar{\lambda}) - \nabla(\bar{\lambda}_1)\| &= \max_{t\in[0,\mathbb{T}]}|\frac{1}{\Gamma(\omega_1)}\int_0^{t}(t_2-g)^{\omega_1-1}\aleph(g,\bar{\lambda}(g)dg \\
&- \frac{1}{\Gamma(\omega_1)}\int_0^{t}(t_1-g)^{\omega_1-1}\aleph(g,\bar{\lambda}_1(g)dg|, \\
&\leq \frac{T^{\omega_1}}{\Gamma(\omega_1+1)}\beta_b|\bar{\lambda}-\bar{\lambda}_1|.
\end{aligned}$$

∇ is hence a contraction. The system (3.1.2) has a unique solution according to the Banach fixed point theorem.

Theorem 3.3: If $(\frac{1-\omega_1}{K(\omega_1)})$, then the system has at least one solution under the continuity of p,q,r,s, and w as well as the second assumption. The value of $\varpi = max\{\varpi_p, \varpi_q, \varpi_r, \varpi_s, \varpi_w\}$ is less than 1.

Proof: Using Krasnosselskii's fixed point theorem, existence results may be demonstrated. $1\Pi = (\Pi_1, \Pi_2, \Pi_3, \Pi_4, \Pi_5)$ is the operator that we define. Let $\;, \Upsilon = (\Upsilon_1, \Upsilon_2, \Upsilon_3, \Upsilon_4, \Upsilon_5)$ as follows:

$$\Pi_1\Omega(t) = S_{K_0} + \frac{1-\omega_1}{K(\omega_1)}p(t,\Omega(t)),$$

$$\Upsilon_1\Omega(t) = \frac{\omega_1}{\Gamma(\omega_1)K(\omega_1)}\int_0^t (t-y)^{\omega_1-1}p(y,\Omega(y))dy,$$

$$\Pi_2\Omega(t) = V_{K_0} + \frac{1-\omega_1}{K(\omega_1)}q(t,\Omega(t)),$$

$$\Upsilon_2\Omega(t) = \frac{\omega_1}{\Gamma(\omega_1)K(\omega_1)}\int_0^t (t-y)^{\omega_1-1}q(y,\Omega(y))dy,$$

$$\Pi_3\Omega(t) = I_{K_0} + \frac{1-\omega_1}{K(\omega_1)}r(t,\Omega(t)),$$

$$\Upsilon_3\Omega(t)=\frac{\omega_1}{\Gamma(\omega_1)K(\omega_1)}\int_0^t(t-y)^{\omega_1-1}r(y,\Omega(y))dy,$$

$$\Pi_4\Omega(t)=J_{K_0}+\frac{1-\omega_1}{K(\omega_1)}s(t,\Omega(t)),$$

$$\Upsilon_4\Omega(t)=\frac{\omega_1}{\Gamma(\omega_1)K(\omega_1)}\int_0^t(t-y)^{\omega_1-1}s(y,\Omega(y))dy,$$

$$\Pi_5\Omega(t)=R_{K_0}+\frac{1-\omega_1}{K(\omega_1)}w(t,\Omega(t)),$$

$$\Upsilon_5\Omega(t)=\frac{\omega_1}{\Gamma(\omega_1)K(\omega_1)}\int_0^t(t-y)^{\omega_1-1}w(y,\Omega(y))dy.$$

Where as $\Omega(t)=S_K(t),V_K(t),I_K(t),J_K(t),R_K(t)$,$\Omega(y)=S_K(y),V_K(y),I_K(y),J_K(y),R_K(y)$ and $\Omega=(S_K,V_K,I_K,J_K,R_K)$. For any $\Omega,(\overline{S_K},\overline{V_K},\overline{I_K},\overline{J_K},\overline{R_K})\in B$,We have;

$$|\Pi_1(t,\Omega(t))-\Pi_1(\bar{t},\overline{\Omega(t)})|.$$

$$\leq(\frac{1-\omega_1}{K(\omega_1)})\varpi_p[|S_K-\overline{S_K}|+|V_K-\overline{V_K}|+|I_K-\overline{I_K}|+|J_K-\overline{J_K}|+|R_K-\overline{R_K}|],$$

$$\|\Pi_2(t,\Omega(t))-\Pi_2(\bar{t},\overline{\Omega(t)})\|.$$

$$\leq(\frac{1-\omega_1}{K(\omega_1)})\varpi_q[|S_K-\overline{S_K}|+|V_K-\overline{V_K}|+|I_K-\overline{I_K}|+|J_K-\overline{J_K}|+|R_K-\overline{R_K}|],$$

$$\|\Pi_3(t,\Omega(t))-\Pi_3(\bar{t},\overline{\Omega(t)})\|.$$

$$\leq(\frac{1-\omega_1}{K(\omega_1)})\varpi_r[|S_K-\overline{S_K}|+|V_K-\overline{V_K}|+|I_K-\overline{I_K}|+|J_K-\overline{J_K}|+|R_K-\overline{R_K}|],$$

$$\|\Pi_4(t,\Omega(t))-\Pi_4(\bar{t},\overline{\Omega(t)})\|.$$

$$\leq(\frac{1-\omega_1}{K(\omega_1)})\varpi_s[|S_K-\overline{S_K}|+|V_K-\overline{V_K}|+|I_K-\overline{I_K}|+|J_K-\overline{J_K}|+|R_K-\overline{R_K}|],$$

$$\|\Pi_5(t,\Omega(t))-\Pi_5(\bar{t},\overline{\Omega(t)})\|.$$

$$\leq(\frac{1-\omega_1}{K(\omega_1)})\varpi_w[|S_K-\overline{S_K}|+|V_K-\overline{V_K}|+|I_K-\overline{I_K}|+|J_K-\overline{J_K}|+|R_K-\overline{R_K}|].$$

Thus;

$$\|\Pi(t),\Omega(t)-\Pi(\bar{t},\overline{\Omega(t)})\|.$$

$$\leq(\frac{1-\omega_1}{K\omega_1})[\|\Omega-(\overline{S_K},\overline{V_K},\overline{I_K},\overline{J_K},\overline{R_K})\|].$$

It demonstrates that Π is a contraction, and the definition of closed subset B of Ω is ;

$$B = \Omega \in \Omega : \|\Omega\| \leq r, r > 0$$

Where; $\Omega = S_K, V_K, I_K, J_K, R_K$. Given any $\Omega \in B$, the proof that Υ is compact and continuous is as follows;

$$\|\Upsilon_1(\Omega)\| \max_{t\in[0,T]} \frac{\omega_1}{\Gamma(\omega_1)K(\omega_1)} \int_0^t (t-y)^{\omega_1-1} p(y,\Omega(y))dy$$

$$\leq \frac{T^{\omega_1}}{\Gamma(\omega_1)K(\omega_1)}[D_p\|A\| + E_p\|A\| + F_p],$$

Similarly we can find $\Upsilon_2(\Omega), \Upsilon_3(\Omega), \Upsilon_4(\Omega), \Upsilon_5(\Omega)$ Thus;

$$\|\Upsilon(\Omega)\| \leq T^{\omega_1} \frac{[(D_1+E_1)r+F_1]}{K(\omega_1)\Gamma(\omega_1)} = \Delta.$$

Where; $D_1 = D_p + D_q + D_r + D_s + D_w$, $E_1 = E_p + E_q + E_r + E_s + E_w$, $F_1 = F_p + F_q + F_r + F_s + F_w$. Hence, we shall demonstrate that Π is absolutely continuous after proving that it is bounded. Assuming that $t_1 < t_2 \in [0,T]$, take into;

$$|\Upsilon_1(\Omega)(t_2) - \Upsilon_1(\Omega)(t_1)| = \frac{\omega_1}{\Gamma(\omega_1)K(\omega_1)} \times |\int_0^{t_2} (t_2-y)^{\omega_1-1} p(y,\Omega(y))dy$$

$$-\frac{\omega_1}{\Gamma(\omega_1)K(\omega_1)} \times \int_0^{t_1} (t_1-y)^{\omega_1-1} p(y,\Omega(y))dy|,$$

$$\leq \frac{\omega_1}{\Gamma(\omega_1)K(\omega_1)}[\int_0^{t_2} (t_2-y)^{\omega_1-1} - \int_0^{t_1} (t_2-y)^{\omega_1-1}]((D_p+E_p))r + F_p dg$$

$$\leq \frac{((D_p+E_p))r+F_p}{K(\omega_1)\Gamma(\omega_1)}[t_2^{\omega_1} - t_1^{\omega_1}].$$

$$|\Upsilon_2(\Omega)(t_2) - \Upsilon_2(\Omega)(t_1)| \leq \frac{((D_q+E_q))r+F_q}{K(\omega_1)\Gamma(\omega_1)}[t_2^{\omega_1} - t_1^{\omega_1}],$$

$$|\Upsilon_3(\Omega)(t_2) - \Upsilon_3(\Omega)(t_1)| \leq \frac{((D_r+E_r))r+F_r}{K(\omega_1)\Gamma(\omega_1)}[t_2^{\omega_1} - t_1^{\omega_1}],$$

$$|\Upsilon_4(\Omega)(t_2) - \Upsilon_4(\Omega)(t_1)| \leq \frac{((D_s+E_s))r+F_s}{K(\omega_1)\Gamma(\omega_1)}[t_2^{\omega_1} - t_1^{\omega_1}],$$

$$|\Upsilon_5(\Omega)(t_2) - \Upsilon_5(\Omega)(t_1)| \leq \frac{((D_w+E_w))r+F_w}{K(\omega_1)\Gamma(\omega_1)}[t_2^{\omega_1} - t_1^{\omega_1}].$$

Consequently, Υ is relatively compact and has a single solution.

3.4. Solutions' positivity and bounded ness

Assuming that they include relevant real-world scenarios, we examine the requirements that guarantee the solutions of the suggested model are positive in order to show that they are logical and limited. In light of this, we have with the usual:

$$\|\Phi\|_\infty = \sup_{t\in(D)_\Phi} |\Phi(t)|.$$

Hence, D_Φ denotes the domain of Φ. This norm indicates that $S_K(t)$ has;

$${}^{C}\mathbb{D}_t^{\omega_1} S_K(t) = \tau + \beta_1 V_K + \beta_2 R_K - (\mu_1 K\phi_1 + \mu_2 K\phi_2 + \theta_1)S_K,$$

$$= -(\mu_1 K\phi_1 + \mu_2 K\phi_2 + \theta_1)S_K.$$

When it comes to the usual derivative, we have;

$$S_K(t) \geq S_K^0 e^{-(\mu_1 K\phi_1 + \mu_2 K\phi_2 + \theta_1)t}, \ \forall\, t \ \geq \ -\varpi.$$

As for $V_K(t)$;

$${}^{C}\mathbb{D}_t^{\omega_1} V_K = \varepsilon S_K - (\omega + \mu_3 K\phi_1 + \mu_4 K\phi_2 + \beta_1)V_K,$$

$$\geq -(\omega + \mu_3 K\phi_1 + \mu_4 K\phi_2 + \beta_1)V_K.$$

When it comes to the usual derivative, we have;

$$V_K(t) \geq V_K^0 e^{-(\omega + \mu_3 K\phi_1 + \mu_4 K\phi_2 + \beta_1)t}, \ \forall\, t \ \geq \ -\varpi.$$

As for $I_K(t)$;

$${}^{C}\mathbb{D}_t^{\omega_1} I_K(t) = \mu_1 K S_K \phi_1 + \mu_3 K V_K \phi_1 - \theta_2 I_K,$$

$$\geq -(\theta_2)I_K.$$

When it comes to the usual derivative, we have;

$$I_K(t) \geq I_K^0 e^{-(\theta_2)t}, \ \forall\, t \ \geq \ -\varpi.$$

As for $J_K(t)$;

$${}^{C}\mathbb{D}_t^{\omega_1} J_K(t) = \mu_2 K S_K \phi_2 + \mu_4 K V_K \phi_2 - \theta_3 J_K,$$

$$\geq -(\theta_3)J_K.$$

When it comes to the usual derivative, we have;

$$J_K(t) \geq J_K^0 e^{-(\theta_3)t}, \ \forall\, t \ \geq \ -\varpi.$$

As for $R_K(t)$;

$${}^{C}\mathbb{D}_t^{\omega_1} R_K(t) = \mu_5 I_K + \mu_6 J_K - (\omega + \beta_2)R_K,$$

$$\geq -(\omega + \beta_2)R_K.$$

When it comes to the usual derivative, we have;

$$R_K(t) \geq R_K^0 e^{-(\omega+\beta_2)t}, \;\; \forall\, t \;\geq\; -\varpi.$$

Theorem 3.4: In R_+^5, the proposed model is unique and limited by the beginning circumstances.
Proof: Here, we used the approach outlined in (Lin, 2007).

$${}^C\mathbb{D}_t^{\omega_1} S_K(t) = \tau + \beta_1 V_K + \beta_2 R_K \quad \geq \;\; 0,$$

$${}^C\mathbb{D}_t^{\omega_1} V_K = \varepsilon S_K \quad \geq \;\; 0,$$

$${}^C\mathbb{D}_t^{\omega_1} I_K(t) = \mu_1 K S_K \phi_1 + \mu_3 K V_K \phi_1 \quad \geq \;\; 0,$$

$${}^C\mathbb{D}_t^{\omega_1} J_K(t) = \mu_2 K S_K \phi_2 + \mu_4 K V_K \phi_2 \quad \geq \;\; 0,$$

$${}^C\mathbb{D}_t^{\omega_1} R_K(t) = \mu_5 I_K + \mu_6 J_K \quad \geq \;\; 0.$$

Above equation demonstrates that the domain R_+^5 stays positive set and unchanged.

3.5. Examination of global stability

The Lyapunov method and Lasalle invariance show that examining global stability identifies the prerequisites for eradicating disease. By using the Lyapunov technique, the global stability analysis gives the conditions needed to eradicate sickness.

3.6. Test of the first derivative

Theorem 3.5: The $S_K V_K I_K J_K R_K$ model's attain global asymptotic stability if $R_0 > 1$ on endemic equilibrium points .
Proof: Following the application of the Lyapunov function we have:

$$\frac{dL}{dt} = (\frac{S_K - S_K^\bullet}{S_K})(\tau + \beta_1 V_K + \beta_2 R_K - (\mu_1 K\phi_1 + \mu_2 K\phi_2 + \theta_1) S_K) + (\frac{V_K - V_K^\bullet}{V_K})(\varepsilon S_K$$

$$-(\omega + \mu_3 K\phi_1 + \mu_4 K\phi_2 + \beta_1) V_K) + (\frac{I_K - I_K^\bullet}{I_K})(\mu_1 K S_K \phi_1 + \mu_3 K V_K \phi_1 - \theta_2 I_K) +$$

$$(\frac{J_K - J_K^\bullet}{J_K})(\mu_2 K S_K \phi_2 + \mu_4 K V_K \phi_2 - \theta_3 J_K) + (\frac{R_K - R_K^\bullet}{R_K})(\mu_5 I_K + \mu_6 J_K - (\omega + \beta_2) R_K)$$

Setting up $S_K = S_K - S_K^\bullet, \;\; V_K = V_K - V_K^\bullet, \;\; I_K = I_K - I_K^\bullet,, \;\; J_K = J_K - J_K^\bullet, \;\; R_K = R_K - R_K^\bullet$ Results in.

$$\frac{dL}{dt} = (\frac{S_K - S_K^\bullet}{S_K})(\tau + \beta_1 (V_K - V_K^\bullet) + \beta_2 (R_K - R_K^\bullet) - (\mu_1 K\phi_1 + \mu_2 K\phi_2)(S_K - S_K^\bullet))$$

$$+(\frac{V_K - V_K^\bullet}{V_K})(\varepsilon (S_K - S_K^\bullet) - (\omega + \mu_3 K\phi_1 + \mu_4 K\phi_2)(V_K - V_K^\bullet)) + (\frac{I_K - I_K^\bullet}{I_K})(\mu_1 K(S_K$$

$$-S_K^\bullet)\phi_1 + \mu_3 K(V_K - V_K^\bullet)\phi_1 - \theta_2 (I_K - I_K^\bullet)) + (\frac{J_K - J_K^\bullet}{J_K})(\mu_2 K(S_K - S_K^\bullet)\phi_2 + \mu_4 K(V_K$$

$$-V_K^\bullet)\phi_2 - \theta_3 (J_K - J_K^\bullet)) + (\frac{R_K - R_K^\bullet}{R_K})(\mu_5 (I_K - I_K^\bullet) + \mu_6 (J_K - J_K^\bullet) - (\omega)(R_K - R_K^\bullet))$$

The above can be put in the following order:

$$\frac{dL}{dt}=\tau-\tau\frac{S_K^\bullet}{S_K}+\beta_1V_K-\beta_1V_K\frac{S_K^\bullet}{S_K}-\beta_1V_K^\bullet+\beta_1V_K^\bullet\frac{S_K^\bullet}{S_K}+\beta_2R_K-\beta_2R_K\frac{S_K^\bullet}{S_K}-\beta_2R_K^\bullet$$

$$+\beta_2R_K^\bullet\frac{S_K^\bullet}{S_K}-\mu_1K\phi_1\frac{(S_K-S_K^\bullet)^2}{S_K}+\mu_2K\phi_2\frac{(S_K-S_K^\bullet)^2}{S_K}+\theta\frac{(S_K-S_K^\bullet)^2}{S_K}+\varepsilon S_K$$

$$-\varepsilon S_K\frac{V_K^\bullet}{V_K}-\varepsilon S_K^\bullet+\varepsilon S_K^\bullet\frac{V_K^\bullet}{V_K}-\omega\frac{(V_K-V_K^\bullet)^2}{V_K}-\phi_1\frac{(V_K-V_K^\bullet)^2}{V_K}-\mu_4K\phi_2\frac{(V_K-V_K^\bullet)^2}{V_K}$$

$$-\omega\frac{(R_K-R_K^\bullet)^2}{R_K}-\beta_2\frac{(R_K-R_K^\bullet)^2}{R_K}-\beta_1\frac{(V_K-V_K^\bullet)^2}{V_K}+\mu_1KS_K-\mu_1KS_K\frac{I_K^\bullet}{I_K}$$

$$-\mu_1KS_K^\bullet+\mu_1KS_K^\bullet\frac{I_K^\bullet}{I_K}+\mu_3K\phi_1V_K-\mu_3K\phi_1V_K\frac{I_K^\bullet}{I_K}-\mu_3K\phi_1V_K^\bullet+\mu_3K\phi_1V_K^\bullet\frac{I_K^\bullet}{I_K}$$

$$-\theta_2\frac{(I_K-I_K^\bullet)^2}{I_K}+\mu_2\phi_2KS_K-\mu_2\phi_2KS_K\frac{J_K^\bullet}{J_K}-\mu_2\phi_2KS_K^\bullet+\mu_2\phi_2KS_K^\bullet\frac{J_K^\bullet}{J_K}$$

$$+\mu_4\phi_2KV_K-\mu_4\phi_2KV_K\frac{J_K^\bullet}{J_K}-\mu_4\phi_2KV_K^\bullet+\mu_4\phi_2KV_K^\bullet\frac{J_K^\bullet}{J_K}-\theta_3\frac{(J_K-J_K^\bullet)^2}{J_K}$$

$$+\mu_5I_K-\mu_5I_K\frac{R_K^\bullet}{R_K}-\mu_5I_K^\bullet+\mu_5I_K^\bullet\frac{R_K^\bullet}{R_K}+\mu_6J_K-\mu_6J_K\frac{R_K^\bullet}{R_K}-\mu_6J_K^\bullet+\mu_6J_K^\bullet\frac{R_K^\bullet}{R_K}.$$

In short, the above may be demonstrated as:

$$\frac{dL}{dt}=F_1-F_2.$$

Where;

$$F_1=\tau-+\beta_1V_K-\beta_1V_K\frac{S_K^\bullet}{S_K}+\beta_1V_K^\bullet\frac{S_K^\bullet}{S_K}+\beta_2R_K+\beta_2R_K^\bullet\frac{S_K^\bullet}{S_K}+\mu_2K\phi_2\frac{(S_K-S_K^\bullet)^2}{S_K}$$

$$+\theta\frac{(S_K-S_K^\bullet)^2}{S_K}+\varepsilon S_K+\varepsilon S_K^\bullet\frac{V_K^\bullet}{V_K}+\mu_1KS_K+\mu_1KS_K^\bullet\frac{I_K^\bullet}{I_K}+\mu_3K\phi_1V_K+\mu_3K\phi_1V_K^\bullet\frac{I_K^\bullet}{I_K}$$

$$+\mu_2\phi_2KS_K+\mu_2\phi_2KS_K^\bullet\frac{J_K^\bullet}{J_K}+\mu_4\phi_2KV_K+\mu_4\phi_2KV_K^\bullet\frac{J_K^\bullet}{J_K}+\mu_5I_K+\mu_5I_K^\bullet\frac{R_K^\bullet}{R_K}+\mu_6J_K.$$

And;

$$F_2=\tau\frac{S_K^\bullet}{S_K}+\beta_1V_K\frac{S_K^\bullet}{S_K}+\beta_1V_K^\bullet+\beta_2R_K\frac{S_K^\bullet}{S_K}+\beta_2R_K^\bullet+\mu_1KS_K^\bullet+\mu_2\phi_2KS_K^\bullet$$

$$+\mu_1K\phi_1\frac{(S_K-S_K^\bullet)^2}{S_K}+\varepsilon S_K\frac{V_K^\bullet}{V_K}+\varepsilon S_K^\bullet+\omega\frac{(V_K-V_K^\bullet)^2}{V_K}+\mu_3K\phi_1\frac{(V_K-V_K^\bullet)^2}{V_K}$$

$$+\mu_4K\phi_2\frac{(V_K-V_K^\bullet)^2}{V_K}+\beta_1\frac{(V_K-V_K^\bullet)^2}{V_K}+\mu_1KS_K\frac{I_K^\bullet}{I_K}+\mu_3K\phi_1V_K\frac{I_K^\bullet}{I_K}+\mu_3K\phi_1V_K^\bullet$$

$$+\theta_2\frac{(I_K-I_K^{\bullet})^2}{I_K}+\mu_2\phi_2KS_K\frac{J_K^{\bullet}}{J_K}+\mu_4\phi_2KV_K\frac{J_K^{\bullet}}{J_K}+\mu_4\phi_2KV_K^{\bullet}+\theta_3\frac{(J_K-J_K^{\bullet})^2}{J_K}$$

$$+\mu_5I_K\frac{R_K^{\bullet}}{R_K}+\mu_5I_K^{\bullet}+\mu_6J_K\frac{R_K^{\bullet}}{R_K}+\mu_6J_K^{\bullet}+\omega\frac{(R_K-R_K^{\bullet})^2}{R_K}+\beta_2\frac{(R_K-R_K^{\bullet})^2}{R_K}$$

It is concluded $F_1 < F_2$ this yields $\frac{dL}{dt} < 0$; however when $S_K = S_K^*,\ V_K = V_K^*,\ I_K = I_K^*,\ J_K = J_K^*,\ R_K = R_K^*$.

$$0 = F_1 - F_2 \implies \frac{dL}{dt} = 0.$$

$$\{(S_K^{\bullet},\ V_K^{\bullet},\ I_K^{\bullet},\ J_K^{\bullet},\ R_K^{\bullet})\ \in\ \Phi\ :\ \frac{dL}{dt} = 0\}.$$

The model is globally asymptotically stable, which is consistent with Lasalle's invariance study.

4. Computational Analysis with Fractional Operator

We provide a Newton polynomial-based numerical method [18] for the suggested model. To keep things simple, :

$$\begin{aligned}
{}^{C}\mathbb{D}_t^{\omega_1}S_K &= S_{K_1}(t,S_K),\\
{}^{C}\mathbb{D}_t^{\omega_1}V_K &= V_{K_1}(t,V_K),\\
{}^{C}\mathbb{D}_t^{\omega_1}I_K &= I_{K_1}(t,I_K),\\
{}^{C}\mathbb{D}_t^{\omega_1}J_K &= J_{K_1}(t,J_K),\\
{}^{C}\mathbb{D}_t^{\omega_1}R_K &= R_{K_1}(t,R_K).
\end{aligned}\tag{11}$$

Where;

$$S_{K_1}(t,S_K) = \tau+\beta_1V_K+\beta_2R_K-(\mu_1K\phi_1+\mu_2K\phi_2+\theta_1)S_K,$$

$$V_{K_1}(t,V_K) = \varepsilon S_K-(\omega+\mu_3K\phi_1+\mu_4K\phi_2+\beta_1)V_K,$$

$$I_{K_1}(t,I_K) = \mu_1KS_K\phi_1+\mu_3KV_K\phi_1-\theta_2I_K,$$

$$J_{K_1}(t,J_K) = \mu_2KS_K\phi_2+\mu_4KV_K\phi_2-\theta_3J_K,$$

$$R_{K_1}(t,R_K) = \mu_5I_K+\mu_6J_K-(\omega+\beta_2)R_K.$$

Using a fractional integral and a power law kernel, we can get;

$$S_K(t_m+1) = S_K(0)+\frac{1}{\Gamma(\omega_1)}\sum_{\mathbb{M}}^{m}\int_{t_{\mathbb{M}}}^{t_{\mathbb{M}+1}}S_{K_1}(t,S_K)\vartheta^{1-\chi}(t_{m+1}-\vartheta)^{\omega_1-1}d\vartheta.$$

Replacing Newton Polynomial into above equations :

$$\begin{aligned}
S_K(t_m+1) \;=\;& S_K(0)+\frac{1}{\Gamma(\omega_1)}\sum_{\mathbb{M}}^{m} S_{K_1}(t_{\mathbb{M}-2},S_K^{\mathbb{M}-2})t_{\mathbb{M}-2}^{1-\chi}\int_{t_{\mathbb{M}}}^{t_{\mathbb{M}+1}}(t_{m+1}-\vartheta)^{\omega_1-1}d\vartheta+\\
&\frac{1}{\Gamma(\omega_1)}\sum_{\mathbb{M}}^{m}\frac{1}{\Delta t}\{t_{\mathbb{M}-1}^{1-\chi}S_{K_1}(t_{\mathbb{M}-1},S_K^{\mathbb{M}-1})-t_{\mathbb{M}-2}^{1-\chi}S_{K_1}(t_{\mathbb{M}-2},S_K^{\mathbb{M}-2})\}+\\
&\int_{t_{\mathbb{M}}}^{t_{\mathbb{M}+1}}(\vartheta-t_{\mathbb{M}-2})(t_{m+1}-\vartheta)^{\omega_1-1}d\vartheta+\frac{1}{\Gamma(\omega_1)}\sum_{\mathbb{M}}^{m}\frac{1}{2\Delta t^2}\{t_{\mathbb{M}}^{1-\chi}S_{K_1}(t_{\mathbb{M}},S_K^{\mathbb{M}})+\\
&-2t_{\mathbb{M}-1}^{1-\chi}S_{K_1}(t_{\mathbb{M}-1},S_K^{\mathbb{M}-1})+t_{\mathbb{M}-2}^{1-\chi}S_{K_1}(t_{\mathbb{M}-2},S_K^{\mathbb{M}-2})\}\\
&\int_{t_{\mathbb{M}}}^{t_{\mathbb{M}+1}}(\vartheta-t_{\mathbb{M}-2})(\vartheta-t_{\mathbb{M}-1})(t_{m+1}-\vartheta)^{\omega_1-1}d\vartheta.
\end{aligned} \tag{12}$$

The integral calculation can be expressed as:

$$\int_{t_{\mathbb{M}}}^{t_{\mathbb{M}+1}}(t_{m+1}-\vartheta)^{\omega_1-1}d\vartheta=\frac{(\Delta t)^{\omega_1}}{\omega_1}\left((m-\mathbb{M}+1)^{\omega_1}-(m-\mathbb{M})^{\omega_1}\right),$$

$$\int_{t_{\mathbb{M}}}^{t_{\mathbb{M}+1}}(\vartheta-t_{\mathbb{M}-2})(t_{m+1}-\vartheta)^{\omega_1-1}d\vartheta=\frac{(\Delta t)^{\omega_1+1}}{\omega_1(\omega_1+1)}\{(m-\mathbb{M}+1)^{\omega_1}(m-\mathbb{M}+3+2\omega_1)$$

$$-(m-\mathbb{M})^{\omega_1}(m-\mathbb{M}+3+3\omega_1)\},$$

$$\int_{t_{\mathbb{M}}}^{t_{\mathbb{M}+1}}(\vartheta-t_{x-2})(\vartheta-t_{\mathbb{M}-1})(t_{m+1}-\vartheta)^{\omega_1-1}d\vartheta=\frac{(\Delta t)^{\omega_1+2}}{\omega_1(\omega_1+1)(\omega_1+2)}\{(m-\mathbb{M}+1)^{\omega_1}$$

$$(2(m-\mathbb{M})^2+(3\omega_1+10)(m-\mathbb{M})+2\omega_1^2+9\omega_1+12)-(m-\mathbb{M})^{\omega_1}$$

$$\times(2(m-\mathbb{M})^2+(5\omega_1+10)(m-\mathbb{M})+6\omega_1^2+18\omega_1+12)\}.$$

Finally,we obtain;

$$S_K(t_m+1)=S_K(0)+\frac{(\Delta t)^{\omega_1}}{\Gamma(\omega_1+1)}\sum_{\mathbb{M}}^{m}t_{\mathbb{M}-2}^{1-\chi}S_{K_1}(t_{\mathbb{M}-2},S_K^{\mathbb{M}-2})C_1+\frac{(\Delta t)^{\omega_1}}{\Gamma(\omega_1+2)}$$

$$\sum_{\mathbb{M}}^{m}\{t_{\mathbb{M}-1}^{1-\chi}S_{K_1}(t_{\mathbb{M}-1},S_K^{\mathbb{M}-1})-t_{\mathbb{M}-2}^{1-\chi}S_{K_1}(t_{\mathbb{M}-2},S_K^{\mathbb{M}-2})\}C_2+\frac{(\Delta t)^{\omega_1}}{\Gamma(\omega_1+3)}$$

$$\sum_{\mathbb{M}}^{m}\{t_{\mathbb{M}}^{1-\chi}S_{K_1}(t_{\mathbb{M}},S_K^{\mathbb{M}})-2t_{\mathbb{M}-1}^{1-\chi}S_{K_1}(t_{\mathbb{M}-1},S_K^{\mathbb{M}-1})+t_{\mathbb{M}-2}^{1-\chi}S_{K_1}(t_{\mathbb{M}-2},S_K^{\mathbb{M}-2})\}C_3.$$

Where;

$$C_1=(m-\mathbb{M}+1)^{\omega_1}-(m-\mathbb{M})^{\omega_1}.$$

$$C_2=(m-\mathbb{M}+1)^{\omega_1}(m-\mathbb{M}+3+2\omega_1)-(m-\mathbb{M})^{\omega_1}(m-\mathbb{M}+3+3\omega_1).$$

$$C_3=(m-\mathbb{M}+1)^{\omega_1}(2(m-\mathbb{M})^2+(3\omega_1+10)(m-\mathbb{M})+2\omega_1^2+9\omega_1+12)$$

$$-(m-\mathbb{M})^{\omega_1}(2(m-\mathbb{M})^2+(5\omega_1+10)(m-\mathbb{M})+6\omega_1^2+18\omega_1+12).$$

5. RESULTS AND DISCUSSION

Here, we created theoretical conclusions and evaluated how well they applied. The parameters values for models is $\tau = 0.08, \omega = 0.07, \varepsilon = 0.6, \mu_1 = 0.06, \mu_2 = 0.04, \mu_3 = 0.02, \mu_4 = 0.002, \mu_5 = 0.3, \mu_6 = 0.6, \kappa_1 = 0.01, \kappa_2 = 0.02, \beta_1 = 0.03, \beta_2 = 0.007, \theta_1 = 0.608, \theta_2 = 0.218, \theta_3 = 0.228$ and initial values are $S_K = 300, V_K = 50, I_K = 1.000, J_K = 70.0000, R_K = 20.000$.

The fractional order introduces memory into the system, meaning that the current rate of change depends on the entire history of the compartment values. For $\omega_1 = 1$, the classical integer-order model is recovered. The system exhibits slower dynamics and a stronger influence of past states, which is particularly relevant for immunological memory, gradual waning of vaccine protection, or delayed public health responses.

To assess the influence of the Caputo fractional derivative on the SVIJR dynamics, we numerically integrate the system for fractional differential equations. The fractional order ω_1 is varied, while all other parameters and initial conditions remain fixed.

The simulations reveal several key impacts of the Caputo operator:

1. **Memory effect:** For $\omega_1 < 1$, the system retains information about its past states. This leads to a slower convergence toward equilibrium compared to the integer-order case ($\omega_1 = 1$). Transient peaks of $I_K(t)$ and $J_K(t)$ are dampened, and the time to reach the endemic steady state increases as ω_1 decreases.
2. **Stability preservation:** The stability properties of the equilibrium points are preserved for all $\omega_1 \in (0, 1]$, confirming that the fractional model does not introduce spurious bifurcations. The disease-free equilibrium remains stable when the effective reproduction number $\mathscr{R}_0 < 1$, and the endemic equilibrium remains stable for $\mathscr{R}_0 > 1$.
3. **Fractional diffusion:** The trajectories in the phase space become smoother and less oscillatory. The 3D phase plots (e.g., *S*–*V*–*I*) show a more gradual approach to the attractor, reflecting the "fractional friction" that reduces instantaneous responsiveness.

These results demonstrate that the Caputo fractional derivative provides a more realistic description of allergic sensitisation and infectious disease dynamics by incorporating immune memory and delayed responses. The numerical simulations confirm that the fractional model remains biologically consistent and numerically stable across the whole range of admissible orders.

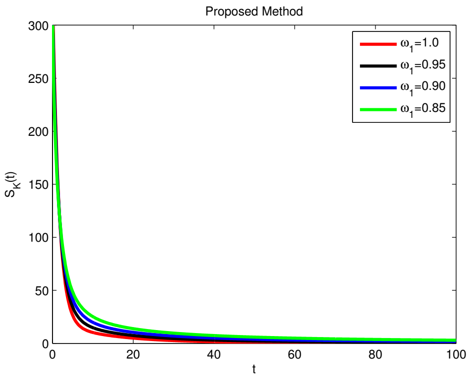

(a) Use of the caputo fractional operator for $S_K(t)$

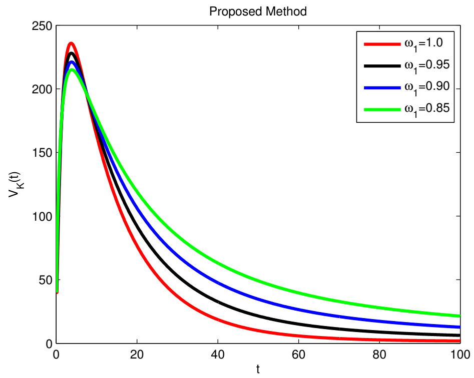

(b) Use of the caputo fractional operator for $V_K(t)$

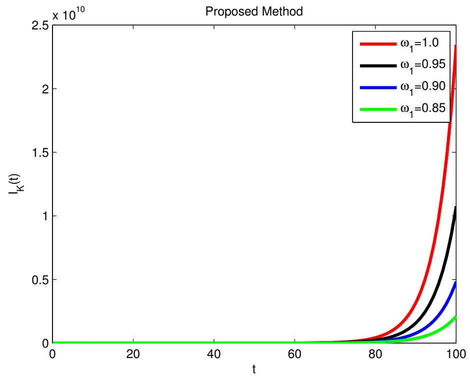

(c) Use of the caputo fractional operator for $I_K(t)$

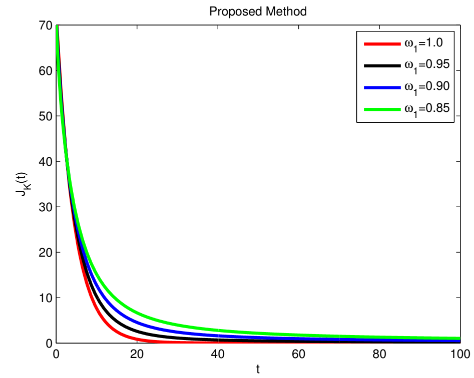

(d) Use of the caputo fractional operator for $J_K(t)$

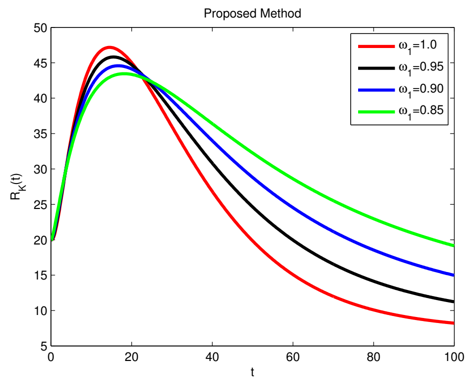

(e) Use of the caputo fractional operator for $R_K(t)$

Figure 3: Behaviour of compartments under Caputo operator.

5.1. Phase plots

In this part, we provide the relation between compartments of the model. The first subplot shows the relationship between susceptible and vaccinated humans. The second plot shows the relationship between the two infected compartments. The third subplot shows the relationship between infected and recovered humans. All trajectories converge to a unique endemic equilibrium, confirming global stability.

Three-dimensional phase portrait of the compartments S , V and I starts at $(300, 50, 1)$ and monotonically approaches the endemic equilibrium without any oscillations, confirming the absence of limit cycles or chaotic behaviour. In Three-dimensional phase portrait of the compartments I, J and R, the initial point quickly moves toward a low-infection equilibrium, demonstrating that recovery dominates and both infection pathways are effectively controlled.

6. Conclusion

This study presents and examines a two-strain $S_K V_K I_K J_K R_K$ epidemic model with immune waning on complex networks and imperfect vaccination. We have determined the conditions for the presence of a coexistence

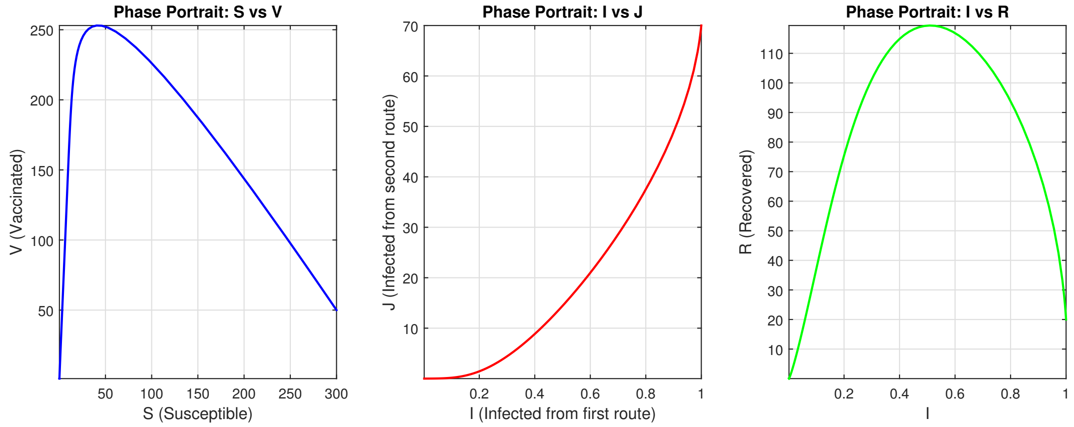

Figure 4: 2d phase plot for compartments of model.

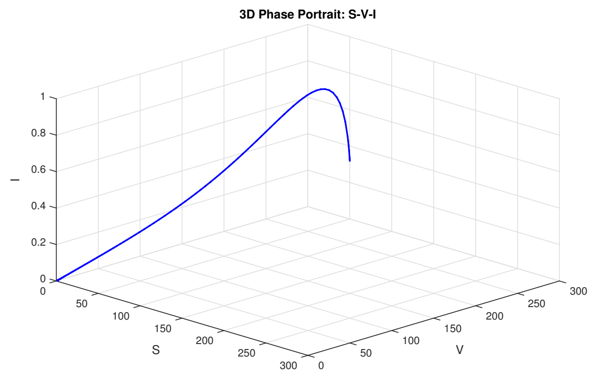

Figure 5: Relation between S,V,I compartments.

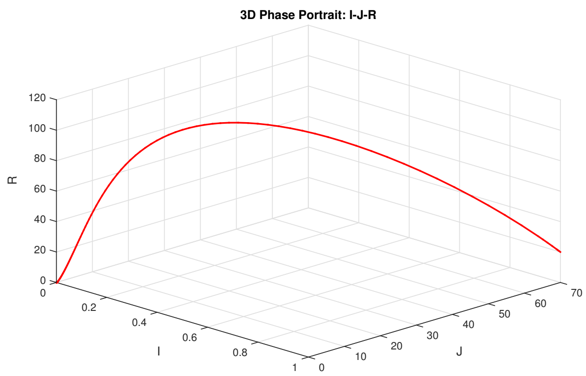

Figure 6: Relation between I,J,R compartments.

equilibrium point and a strain dominance equilibrium point based on LaSalle's invariance principle and the Lyapunov function. Additionally, we have established the conditions necessary to guarantee the four equilibrium points' global state. We first discovered that the proposed epidemic model had four equilibrium points: one coexistence equilibrium point, one disease-free equilibrium point, and two single-strain endemic equilibrium points. After that, it is found that the fundamental reproduction number, represented by $\mathbf{R}_1$ and $\mathbf{R}_2$, is the critical threshold that determines the general spread of the disease and also sensitivity analysis developed. Additionally, the global stability has been examined using the Lyapunov function approach. Asymptotically, the disease-free equilibrium point is stable worldwide. In other words, when $\max\{\mathbf{R}_1, \mathbf{R}_2\} < 1$, the illness would vanish. Additionally, the co-existence equilibrium is global asymptotically stable, which means that when $\min\{\mathbf{R}_1, \mathbf{R}_2\} > 1$, both strains coexist and achieve a positive steady state. We derived the model's existence and distinctiveness including the solution's bounded ness. Lastly, it is clear that the strain with the greatest competitive advantage will have the highest basic reproductive number. Solutions are derived by the advanced tools for the proposed two strain mathematical model. Estimates may also be based on confirmed findings from further research that will aid in understanding the behavior, environmental propagation, early detection process by utilizing numerically simulation using MATLAB coding.

Conflict of Interest

The authors declare that there is no conflict of interest regarding the publication of this manuscript.

Data Availability:

The data used in this study are available upon reasonable request.

Authors' Contributions :

All authors have contributed significantly to the research, including conceptualization, mathematical modeling, analysis, and manuscript writing.

References

[1] Musso, D., & Gubler, D. J. (2016). Zika virus. *Clinical Microbiology Reviews*, 29(3), 487–524.

[2] Rodríguez, J. A. M., et al. (2018). Zika virus: A review to clinicians. *Acta Médica Portuguesa*, 31(4), 227–235.

[3] Ciotti, M., et al. (2020). The COVID-19 pandemic. *Critical Reviews in Clinical Laboratory Sciences*, 57(6), 365–388.

[4] Gershenfeld, N. (1999). *The Nature of Mathematical Modeling*. Cambridge University Press.

[5] Kermack, W. O., & McKendrick, A. G. (1927). A contribution to the mathematical theory of epidemics. *Proceedings of the Royal Society of London. Series A*, 115(772), 700–721.

[6] Abdullah, M., Ahmad, A., Raza, N., Farman, M., & Ahmad, M. (2018). Approximate solution and analysis of smoking epidemic model with Caputo fractional derivatives. *International Journal of Applied and Computational Mathematics*, 4(5), 112.

[7] Farman, M., Ahmad, A., Akgül, A., Saleem, M. U., Rizwan, M., & Ahmad, M. O. (2020). A mathematical analysis and simulation for Zika virus model with time fractional derivative. *Mathematical Methods in the Applied Sciences*.

[8] Ahmad, A., Farman, M., Naik, P. A., Zafar, N., Akgul, A., & Saleem, M. U. (2021). Modeling and numerical investigation of fractional-order bovine babesiosis disease. *Numerical Methods for Partial Differential Equations*, 37(3), 1946-1964.

[9] Abdeljawad, T., Younus, A., Alqudah, M., & Atta, U. (2023). On fuzzy conformable double laplace transform with applications to partial differential equations. *Computer Modeling in Engineering & Sciences*, 134(3), 2163.

[10] Younus, A., Asif, M., Atta, U., Bashir, T., & Abdeljawad, T. (2023). Applications of fuzzy conformable Laplace transforms for solving fuzzy conformable differential equations. *Soft Computing*, 27(13), 8583-8597.

[11] Ahmad, A., Atta, U., Akgül, A., Sattar, S., & Ahmad, M. O. (2025). A study on mathematical modeling and control of leptospirosis transmission dynamics during a hurricane with asymptomatic measures.*Modeling Earth Systems and Environment*, 11(5), 361.

[12] Farman, M., Ahmad, A., Atta, U., Nisar, K. S., & Ghaffar, A. (2025). Hyers Ulam stability and bifurcation control of leptospirosis disease dynamics and preventations: Modeling with singular and non-singular kernels.*PloS one*, 20(3), e0314095.

[13] Teklu, S. W. (2024). Insight into the optimal control strategies on corruption dynamics using fractional order derivatives. *Scientific African*, 23, e02069.

[14] Teklu, S. W. (2023). Analysis of fractional order model on higher institution students' anxiety towards mathematics with optimal control theory. *Scientific Reports*, 13(1), 6867.

[15] Awadalla, M., Alahmadi, J., Cheneke, K. R., & Qureshi, S. (2024). Fractional Optimal Control Model and Bifurcation Analysis of Human Syncytial Respiratory Virus Transmission Dynamics. *Fractal and Fractional*, 8(1), 44.

[16] Padder, A., Almutairi, L., Qureshi, S., Soomro, A., Afroz, A., Hincal, E., & Tassaddiq, A. (2023). Dynamical analysis of generalized tumor model with Caputo fractional-order derivative. *Fractal and Fractional*, 7(3), 258.

[17] Khatri, K., et al. (2022). Multi-strain epidemic models: A review. *Journal of Biological Dynamics*, 16(1), 45–67.

[18] Atangana, A., & Araz, S. İ. (2021). New numerical scheme with Newton polynomial: theory, methods, and applications. *Academic Press*.